Working Report 2014-07

Tunnel Backfill Erosion by Dilute Water

Markus Olin

VTT

March 2014

TUNNEL BACKFILL EROSION BY DILUTE WATER

ABSTRACT

The goal was to estimate smectite release from tunnel backfill due to dilute groundwater pulse during post glacial conditions. The plan was to apply VTT's two different implementations (BESW_D and BESW_S) of well-known model of Neretnieks *et al.* (2009).

It appeared difficult to produce repeatable results using this model in COMSOL 4.2 environment, therefore a semi-analytical approximate approach was applied, which enabled to take into account both different geometry and smectite content in tunnel backfill as compared to buffer case. The results are quite similar to buffer results due to the decreasing effect of smaller smectite content and the increasing effect of larger radius.

Keywords: Smectite, erosion, dilute groundwater, modelling, backfill.

LAIMEIDEN POHJAVESIEN AIKAANSAAMA LOPPUSIJOITUSTUNNELEIDEN TÄYTÖN EROOSIO

TIIVISTELMÄ

Työn tavoite on arvioida smektiitin vapautumista tunnelitäyttöstä postglasiaaliolosuhteiden seurauksena mahdollisesti loppusijoitustiloihin tunkeutuvista laimeista pohjavesistä. Tarkoituksena oli soveltaa kahta eri VTT:n kehittämää toteutustapaa, joilla toteutetaan hyvin tunnettu Neretnieks *et al.* (2009) esittämä malli.

Osoittautui, että tämän mallin avulla on hankala tuottaa tuloksia toistettavasti COMSOL 4.2 :n avulla. Tästä syystä käytettiin puolianalyyttistä likimääräistä lähestymistapaa ja tällä tavalla onnistuttiin huomioimaan sekä puskuri ja tunnelitäytön erilaiset geometriat että erilaiset smektiittipitoisuudet. Tulokset ovat puskurille saatujen tulosten kanssa hyvin samanlaiset, sillä tunnelitäytön suuremmasta geometriasta aiheutuva eroosiomäärän kasvu kompensoitui tunnelitäytteen puskuria alhaisemmalla smektiittipitoisuudella.

Avainsanat: Smektiitti, eroosio, laimea pohjavesi, mallinnus, tunnelitäyttö.

TABLE OF CONTENTS

1 DESCRIPTION AND OBJECTIVES

Erosion by dilute post glacial melt waters is one of the major issues concerning buffer smectite. In the tunnel backfill the smectite content is lower, but anyhow it seems possible that erosion may take place there, too.

Both experiments and modelling have been carried out in Sweden and Finland over the subject during recent years. However, no direct experimental data is available for tunnel backfill materials, and anyhow, it is very difficult to extrapolate laboratory data to full scale and duration of post glacial fresh groundwater pulse. Therefore, some model approach is needed.

The most commonly applied model in this context is presented by Neretnieks *et al.* (2009). The model has no fitting parameters and it is largely based on microscopic level modelling. The model has appeared to be hard to solve, and the origin of these observed difficulties is still open: physics of the model itself or model implementations (mainly on COMSOL Multiphysics platform).

The goal of the work was to estimate tunnel erosion (grams per cross-sectional area of fracture per year or in simpler form grams per length of fracture per year at given fracture aperture) by Neretnieks model (Neretnieks et al. (2009)), which however appeared to be very difficult. Instead of that a simpler approximate approach was developed and applied.

A brief discussion is given below about our two implementations of Neretnieks model and the approximate approach. All results shown here are based on the approximate model.

2 MODELS

Two modelling approaches were applied:

1. Direct application of our implementation - BESW (Smectite Expansion into Seeping Water) on COMSOL Multiphysics: functions in data form, BESW_D, or symbolic approximation, BESW_S - of Neretnieks et al. (2009) model.

2. Approximate calculation method developed at VTT, BESW_A.

Our BESW model is described in details in other reports (Itälä *et al.* (2010), Schatz *et al.* (2013)), therefore only very brief introduction and the different parameterisation compared to buffer are given here. However, the approximate model, BESW_A, was developed during the work, and therefore a more detailed description is given below. An illustration of how different model implementations relate to each other see Appendix C.

2.1 BESW_D and BESW_S models

The original equations in Neretnieks' et al. (2009) model are quite complex including several nested function calls, which makes for example debugging rather difficult (more detailed description given in Appendix A). Therefore, we choose to apply numerical functions in COMSOL Multiphysics instead of implementing the functions directly. In this approach the values of functions are given over a mesh and COMSOL interpolates and extrapolates the function values needed (BESW_D implementation). All functions were carefully tested in Matlab before applying them into COMSOL. To further increase quality all functions were implemented onto symbolic mathematics program Maple, too. The diffusivity of smectite depends in a highly non-linear way on volume fraction of smectite and also salinity. However, it is an open question which dependencies are causing the observed numerical problems. One of the problems is the very narrow front of volume fraction of smectite, ϕ in the region of interest, i.e. $0.001< \phi <0.02$. This must be followed with a very detailed discretisation over the whole geometry especially, if time dependent solution is wanted or with application of some adaptive mesh refinement method.

The model equations given for smectite diffusion by Neretnieks et al. (2009) are a quite complex set of composite functions (see Appendix A for details). Therefore, we tried to fit something not so complicated especially (BESW_S implementation, Appendix B) to the diffusion function of smectite, which behaves non-linearly as function of a salinity (ionic strength) and volume fraction of smectite. In order to enhance numerical computation in COMSOL Multiphysics, we have simplified some functional dependencies. All simplifications are based on relatively simple analytical relations, for which first order partial derivatives are also available.

Our conceptual thinking is sketched in Figures 1 and 2 (first one calculated by BESW_S, and therefore the curve is somewhat smoother than the original one), where the diffusivity of smectite, D_F is shown as a function of ϕ at 0.1 mM salinity. There is a high diffusivity value which is reached at 0.1 mM salinity, when volume fraction ϕ is high enough (> 0.003). At low ϕ values the behaviour appears somewhat more complicated (see Figure 1b for details). The viscosity of water, η is monotonously increasing with increasing volume fraction, and very clear increase starts at $\phi \sim 0.004$. In model simulations, it is assumed that higher salinity pore water is diffusing out of smectite in low salinity groundwater. Therefore, in simulation cases salinity is low at lower (near groundwater-smectite boundary) volume fraction values, and the diffusion profile is similar to Figure 1a.

Therefore, there exist three different zones in the system (Figure 1b):

1. First, the compact or gel like smectite, where relative viscosity is so high that water flow velocity with gel/sol is practically zero: $\phi > 0.005 - 0.01$ depending on criteria (in Figure 1a the limit is set to 20 times the bulk viscosity, but higher limit may be needed at higher groundwater velocity). Note, that faster flowing water penetrates deeper into the smectite, when advection and diffusion induced transport are compared. In our simplified model only diffusion is modelled here.
2. Second, the boundary layer between the two other zones, in which both diffusivity and viscosity change rapidly as a function of ϕ: $\phi \cong 0.002 - 0.01$. In this layer diffusion is assumed to behave as a source term, high enough diffusivity to transport material into and within the zone, and groundwater flow as a main transport mechanism; because both flow velocity and volume fraction have high enough values only here.

   Third, the colloidal smectite, the diffusivity of which is so low that only at very low groundwater velocity diffusion is the dominating transport mechanism: $\phi < 0.002 - 0.003$. In our simplified model no transport is taking place here.

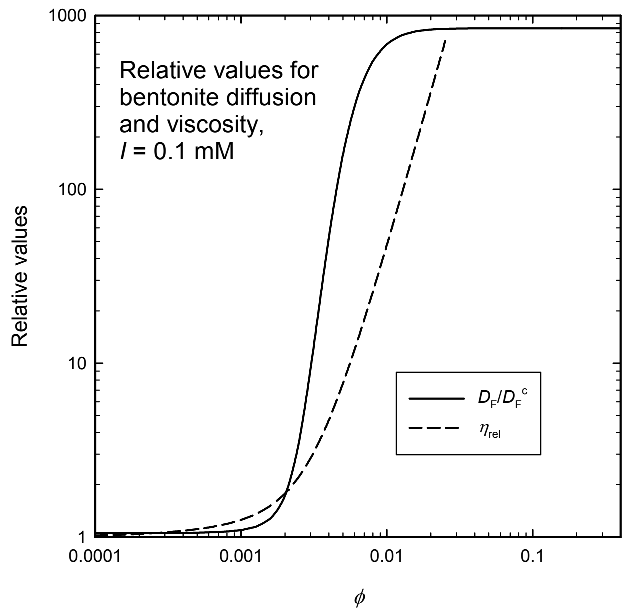

a)

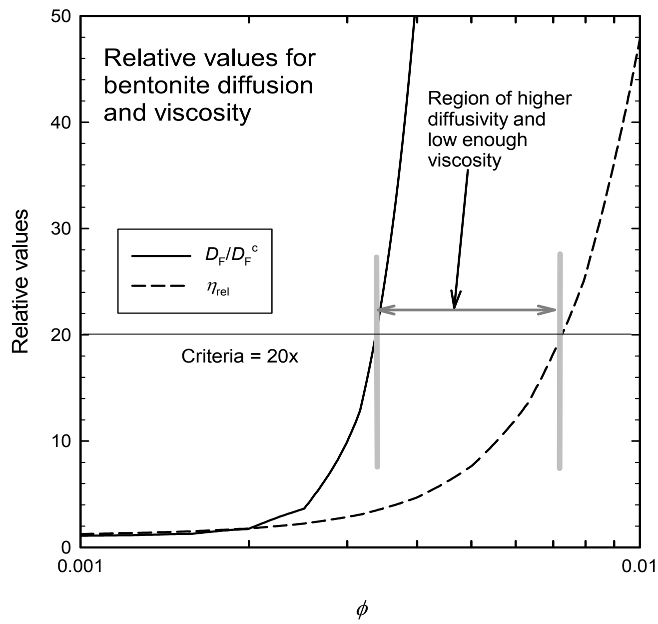

b)

Figure 1. *Relative diffusivity (value one stands for colloidal) of smectite and relative viscosity (value one corresponds free water) as a function of volume fraction of smectite (at salinity 0.1 mM). The diffusivity curve has a distinct turning point, before which diffusivity is low and after which it is high. The location of turning points depends on salinity and is increasing by increasing salinity. In top figure (a) the whole studied range is shown, while in bottom (b) figure the most interesting zone 2 in shown in linear y-axis scale.*

These three zones are sketched also in Figure 2 (the top figure shows buffer case, but just by replacing the buffer by the tunnel, the sketch is relevant to tunnel backfill erosion, too. The main assumption in our simple model is to separate transport in zones one and three so, that the penetration depth determines the mass flux in zone one, and then in the steady state this enables the estimation of depth of zone 3. Finally, depending on the groundwater velocity the penetration depth must be adjusted so that it is possible to transport all released smectite out of the system via zone 3. Detailed description of the approximating, BESW_A, model is given in other reports (Itälä *et al.* (2010), Schatz *et al.* (2013)).

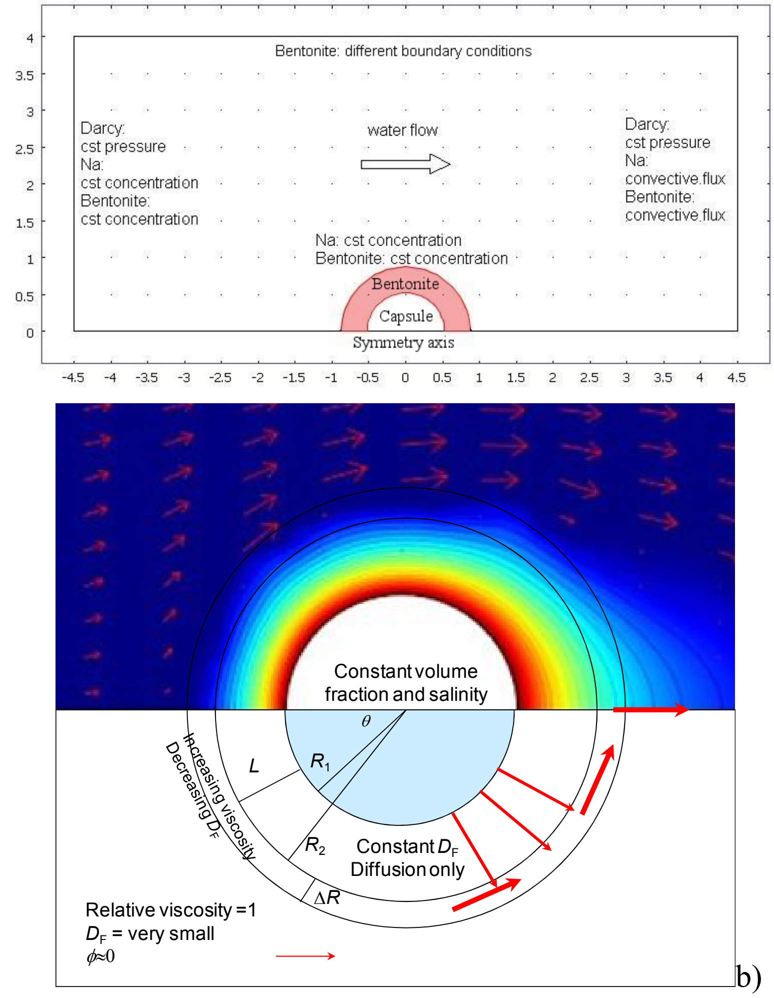

Figure 2. *Sketch of modelling cases in two scales. a) The whole system and boundaries. b) An example result from VTT's earlier modelling (top) and sketch of BESW_A model philosophy (bottom).*

2.2 Approximated Neretnieks' model – BESW_A

Let us consider steady state situation, where smectite has extruded into the fracture and there exists a diffusion profile for salinity: salinity is lower in areas of lower smectite content. At low salinity the diffusion coefficient of smectite is higher than in high salinity pore water. Form Figure 1, we can even conclude that at steady state the diffusivity of smectite has almost constant value from lower smectite threshold content up to high content. At the boundary between the smectite low content edge and free flowing ground water, however, the equations are pretty complicated, but we may assume that this layer is in most conditions rather thin. The reasoning behind this assumption relies on the constant flux at steady state: low diffusivity at low smectite content means high gradient, which especially at the very low smectite content (below 0.003) considered means that the layer must be thin compared to the layer of higher diffusivity.

First approximation is to apply cylindrical coordinate system, and assume smectite diffusing only in radial direction in zone 1, while the groundwater is flowing azimuthally in zone 2. No groundwater flow in layer 1 and no significant transport of smectite in layer 3, where groundwater flows freely around the penetrated smectite zone (1+2).

The steady state solution for diffusion equation in polar coordinates (steady state, assuming approximately constant diffusivity down to volume fraction ϕ_2):

$$\phi = A \ln r + B \tag{1}$$

where r is the radial coordinate, and A and B are coefficients to be fitted on boundary conditions, which are

$$\begin{aligned} \phi(R_1) &= \phi_1 \\ \phi(R_2) &= \phi_2 < \phi_1 \end{aligned} \tag{2}$$

where R_1 is the (inner or source) radius at constant volume fraction (ϕ_1) and R_2 is the (outer) radius at some clearly lower volume fraction (ϕ_2), which value is to be determined later in this analysis. At ϕ_2 and out of distance R_2 the diffusivity is assumed to drop down dramatically, but in many cases most of the diffusion resistance will be in this "constant" diffusivity regime.

Solution fulfilling boundary conditions

$$\phi = \frac{\phi_1 - \phi_2}{\ln(R_1/R_2)}(\ln r - \ln R_2) + \frac{\phi_2 \ln R_1}{\ln(R_1/R_2)} \cong \frac{\phi_1}{\ln(R_1/R_2)}(\ln r - \ln R_2) \tag{3}$$

Diffusion flux at outer radius is therefore

$$j = -D_{\mathrm{F}}^{\mathrm{h}} \left.\frac{\partial \phi}{\partial r}\right|_{r=R_2} \cong \frac{D_{\mathrm{F}}^{\mathrm{h}}}{\ln(R_2/R_1)} \frac{\phi_1}{R_2} \tag{4}$$

Mass flux per metre at inner radius (the quantity to be estimated by our analysis) will be

$$q(R_1) = \rho_s \delta\, j(R_1) = -\rho_s \delta\, D_{\mathrm{F}}^{\mathrm{h}} \left.\frac{\partial \phi}{\partial r}\right|_{r=R_1} = \frac{D_{\mathrm{F}}^{\mathrm{h}}}{\ln(R_2/R_1)} \frac{\rho_s \delta \phi_1}{\mathrm{R}_1} \tag{5}$$

and the total flux

$$Q = 2\pi R \cdot q(R) = -2\pi \rho_s \delta\, D_{\mathrm{F}}^{\mathrm{h}} \left.\frac{\partial \phi}{\partial r}\right|_{r=R} = 2\pi \frac{D_{\mathrm{F}}^{\mathrm{h}} \rho_s \delta \phi_1}{\ln(R_2/R_1)} \tag{6}$$

where ρ_{S} is the specific density of smectite and δ the aperture of the fracture.

The system is determined by R_1, boundary condition, ϕ_1, and aperture of the fracture δ, which are all known and the job to be done is to evaluate R_2 as a function of velocity.

The functional form of dependence between groundwater velocity and penetration depth, $L = R_2 - R_1$, may obtained by the following reasoning:

1. Almost all diffusion resistance of smectite is found in an area of almost constant diffusivity

2. In the area of decreasing diffusivity the flux is though at steady state equal to flux in constant diffusivity area (everything coming in must go out). However, the volume fraction decrease is small, approximately from 0.01 down to 0.002, where the smectite starts to be colloidal. It may be assumed that the concentration difference is almost constant for all cases and therefore the gradient must be very steep due to low diffusivity.

3. In the high volume fraction area the smectite moves only by diffusion and in colloidal area the only transport mechanism is advection, however, the volume fraction there being so low that no effective transport in taking place.

4. Therefore, the only zone where diffusion and advection work together is the narrow boundary layer, where diffusivity increases and relative viscosity decrease rapidly, when going from low volume fraction to higher values. The work to be done is to calculate the width of the layer.

A detailed analysis of all this is outside the scope of this assessment and is planned to be presented elsewhere. Therefore, the following argumentation is more narrative than exact. At steady state diffusive flux is constant independent of the local diffusivity value:

$$D_\mathrm{F}^\mathrm{h} \frac{\phi_1 - \phi_2}{\ln\left(R_2/R_1\right)} = D_2 \frac{\phi_2 - \phi_3}{\ln\left(R_3/R_2\right)} = \frac{D_2 \Delta\phi}{\ln\left(1 + \dfrac{\Delta R}{R_2}\right)} \cong R_2 D_2 \frac{\Delta\phi}{\Delta R} \cong D_\mathrm{F}^\mathrm{h} \frac{\phi_1}{\ln\left(R_2/R_1\right)} \tag{7}$$

where D_2 represents diffusivity in the layer (zone 3) and approximation $\ln\left(1 + \Delta R/R_2\right) \cong \Delta R/R_2$ has been applied. It is easy to solve the layer thickness ΔR

$$\Delta R = R_2 \ln\left(R_2/R_1\right) \frac{D_n}{D_1} \frac{\Delta\phi_n}{\phi_1} = B\left(D\left(\phi\right)\right) \frac{R_2 \ln\left(R_2/R_1\right)}{\phi_1} \tag{8}$$

where B is the coefficient including all other dependencies except the inner and outer radius (R_1 and R_2), and the inner (boundary) volume fraction (ϕ_1). It is possible to present more detailed study about layer thickness by applying the real diffusion function in zone 2, but the dependency in our approximation is factorised as in Equation (8).

Next, we present a simple estimate for mass balance, where the inlet is via diffusive flux and outlet occurs via boundary layer, and depends on volume fraction there, and groundwater velocity:

$$Q = \frac{2\pi D_{\mathrm{F}}^{\mathrm{h}} \rho_{\mathrm{S}} \delta\phi_1}{\ln\left(R_2/R_1\right)} \approx \rho_{\mathrm{S}} \delta\phi_2 v \Delta R \tag{9}$$

By substituting ΔR from Equation (8) we have

$$\frac{D_{\mathrm{F}}^{\mathrm{h}} \rho_{\mathrm{S}} \delta\phi_1}{\ln\left(R_2/R_1\right)} \approx \rho_{\mathrm{S}} \delta\phi_2 v \frac{R_2 \ln\left(R_2/R_1\right)}{\phi_1} \tag{10}$$

which finally gives

$$v \approx \frac{\phi_1^2}{R_2 \left[\ln\left(R_2/R_1\right)\right]^2} \tag{11}$$

where again only geometry and boundary value parameters are retained. Therefore, we will apply following fitting formulae

$$v = A\left(\frac{\phi_1}{\phi_0}\right)^2 \frac{1}{R_2\left[\ln\left(\frac{R_2}{R_1}\right)\right]^2} = A\left(\frac{\phi_1}{\phi_0}\right)^2 \frac{1}{\left(R_1 + L\right)\left[\ln\left(\frac{R_1 + L}{R_1}\right)\right]^2} \tag{12}$$

where A is a fitting parameter, L is the penetration depth of smectite and ϕ_0 is the reference volume fraction i.e. that used in model calculations to be fitted.

2.3 System and parameters

The modelled system is sketched in Figure 2. The size of the system depends on flow velocity, because at highest studied velocity (300 m/a) the assumed penetration depth of smectite is on the order of a metre, while at low velocity (0.1 m/a) the penetration depth may be very high, even about 100 metres. Groundwater and pore water salinities are set to 0.1 and 10 mmol/L, respectively. The boundary value for volume fraction of smectite $\phi_1 = 0.296$. Studied groundwater velocity varies from 0.1 m/a to 315 m/a.

3 RESULTS

3.1 Calculations

The model is fitted to model calculations obtained by KTH (Moreno et al., 2010) and VTT (Itälä et al. 2010). The model results are shown in Table 1 (water velocity, smectite release and penetration depth).

Table 1. *Water velocity, smectite release and penetration depth: KTH, TR-10-64, Table 5-1 (Moreno et al., 2010); and VTT, VTT-R-07924-10, Table 2 (Itälä et al., 2010).*

v (m/a)	KTH release (kg/a/m)	KTH *L* (m)	VTT release (kg/a/m)	VTT *L* (m)
0.1	0.004	34.6	0.017	31.4
0.32	0.006	18.5	0.017	26.7
0.95	0.009	11.5	0.017	19.9
3.15	0.016	7	0.018	16.9
9.45	0.026	4.1	-	-
31.5	0.043	2.1	0.029	5.3
94.5	0.065	1	-	-
315	0.106	0.5	0.088	0.85

From Equation (5) it is possible to calculate the "effective diffusivity" by data given in Table 1. Those results are shown in Table 2. The highest value of smectite diffusivity is about 1.6E-9 m^2/s, and therefore VTT's results are in all cases near that and KTH's results somewhat lower especially at lower groundwater velocities. To be conservative the highest value, 1.6E-9 m^2/s, was chosen for all model calculations of the report.

Table 2. *Calculated effective diffusivity values.*

v (m/a)	KTH DFh (m^2/s)	VTT DFh (m^2/s)
0.1	3.73E-10	1.55E-09
0.32	4.54E-10	1.49E-09
0.95	6.32E-10	1.37E-09
3.15	8.66E-10	1.35E-09
9.45	1.13E-09	
31.5	1.31E-09	1.43E-09
94.5	1.26E-09	
315	1.21E-09	1.51E-09

The observed and fitted (to Equation 10) groundwater velocity values as function of penetration depth for the buffer case: boundary smectite volume fraction 0.4 and radius 0.875 m were applied in the fitting (Figure 3). The fitting parameter A = 76 m^2/s.

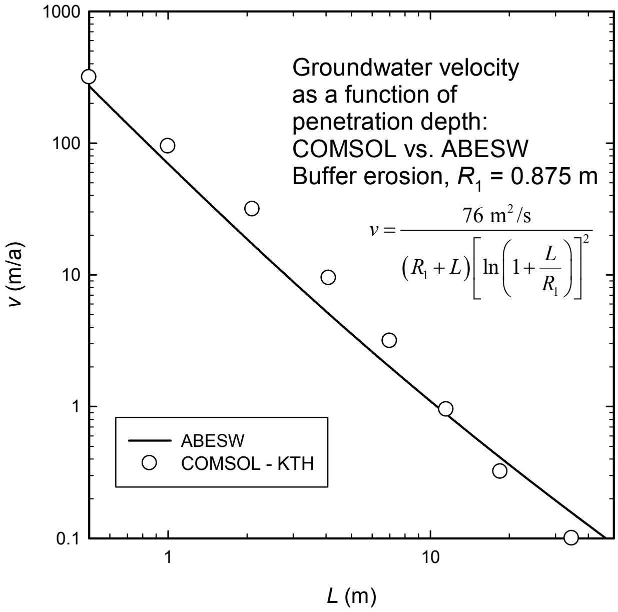

Figure 3. *A fit to our model's Equation 10 using KTH's results. VTT's results would give somewhat different fitting.*

In Figure 4 the velocity is given as function of penetration depth for tunnel backfill, and in Table 3 the values obtained for penetration depth are applied to produce smectite release rate. In Figure 5 the release rates are shown as a function of groundwater velocity in linear and log-log scales.

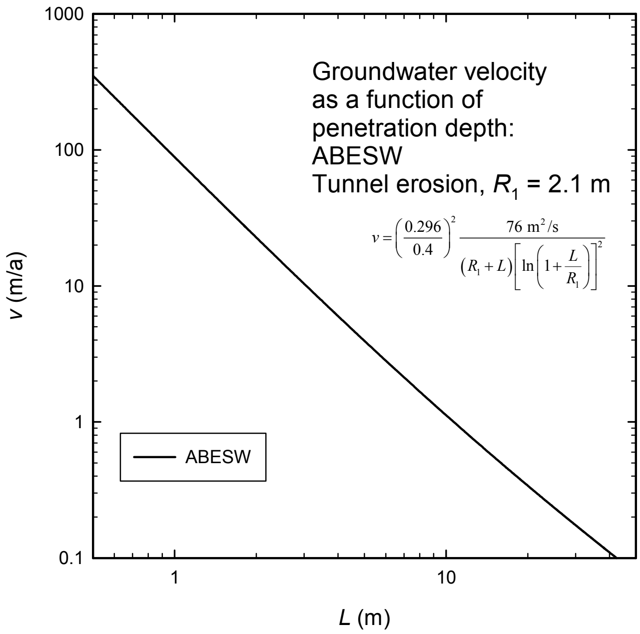

Figure 4. *Like Figure 3, but now the fitted form was applied to tunnel backfill system (larger radius). From the figure it is possible to obtain penetration depth L as a function of velocity (shown in Table 3).*

Table 3. *Final results (penetration depth and release) as a function of velocity for tunnel backfill.*

v (m/a)	*L* (m)	release (kg/m/a)
0.1	42.5	0.0064
0.32	20.8	0.0082
0.95	11	0.0107
3.15	5.6	0.0151
9.45	3.15	0.0214
31.5	1.7	0.0330
94.5	0.96	0.0520
315	0.53	0.0870

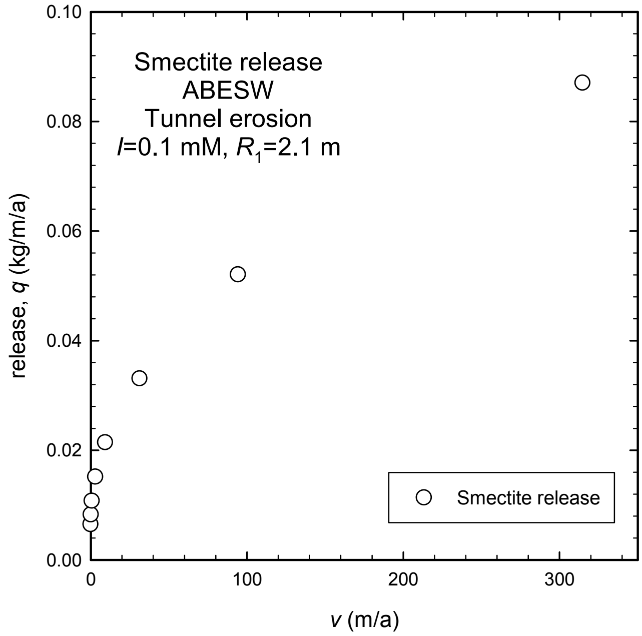

a)

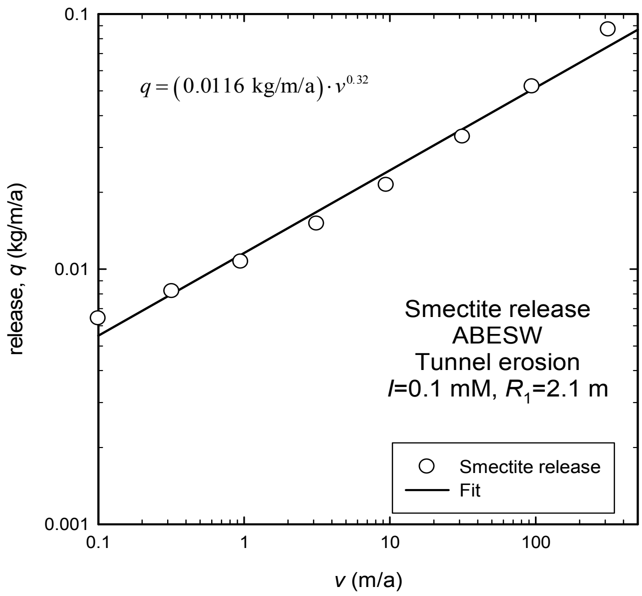

b)

Figure 5. *Smectite release, q, for tunnel erosion as a function of velocity: a) in linear scale and b) in log-log scale (linear fit in log values also given).*

3.2 Discussion

Due to controversial results obtained in COMSOL Multiphysics simulation of both BESW versions (D and S), we were forced to develop an approximate model (BESW_A) to carry out the calculations needed. The BESW_A model, however needed fitting of one parameter in penetration depth as a function of velocity formula (Equation 10), and in this fitting KTH's numerical results were applied.

Some new calculations by both BESW_D and BESW_S models are either going on or planned (November 2011) to be done, but these results will not available for this report.

4 CONCLUSIONS AND SUMMARY

The model of Neretnieks *et al.* (2009) has appeared to be difficult to solve, and therefore semi-analytical approximate approach was applied, which enabled us to take account of both different geometry and smectite content in tunnel backfill compared to buffer case. The results are quite similar to buffer results due to decreasing effect of smaller smectite content and increasing effect of larger radius.

REFERENCES

Itälä A., Seppälä A., Pulkkanen V.-M. & Olin M. 2010. Smectite Expansion into Seeping Water (BESW). VTT-R-07924-10. 20 p.

Neretnieks I., Liu L. & Moreno L. 2009. Mechanisms and models for smectite erosion. TR-09-35. Stockholm, Sweden: SKB - Swedish Nuclear Fuel and Waste Management Co. 174 p.

Moreno L., Neretnieks I., & Liu L. 2010. Modelling of erosion of smectite gel by gel/sol flow. TR-10-64. Stockholm, Sweden: SKB - Swedish Nuclear Fuel and Waste Management Co. 56 p.

Schatz T., Kanerva N., Martikainen J., Sane P,, Olin M., Seppälä A. & Koskinen K. 2013. Buffer Erosion in Dilute Groundwater, Posiva Report 2012-44. Posiva Oy.

Appendix A: The complete set of equations in Neretnieks' model

The mutual dependencies of the model variables c (sodium concentration), ϕ (volume fraction of smectite) and p (pressure) are sketched in Figure A1. The nomenclature and fixed values of parameters are collected in Table A1.

Advection-diffusion equation for sodium ions is:

$$\frac{\partial c(\mathbf{x},t)}{\partial t} = \nabla\cdot\left(D\left(\phi(\mathbf{x},t)\right)\nabla c(\mathbf{x},t)\right) - \mathbf{u}(\mathbf{x},t)\nabla c(\mathbf{x},t)$$

where D is the diffusion coefficient for sodium in water, $\mathbf{u}$ is the Darcy velocity from pressure field, and $\mathbf{x}$ and t are the space and time coordinates, respectively. Diffusion coefficient varies as a function of volume fraction of smectite

$$D(\mathbf{x},t) = D_0\left(1-\phi(\mathbf{x},t)\right)^{1.6}$$

The equation for smectite expansion:

$$\frac{\partial \phi(\mathbf{x},t)}{\partial t} = \nabla\cdot\left(D_{\mathrm{F}}\left(c(\mathbf{x},t),\phi(\mathbf{x},t)\right)\nabla\phi(\mathbf{x},t)\right) - \mathbf{u}(\mathbf{x},t)\cdot\nabla\phi(\mathbf{x},t)$$

The diffusivity is given as the ratio of the sum of the energy of these smectite particles χ and the friction coefficient f between particles and water

$$D_{\mathrm{F}}(\mathbf{x},t) = D_{\mathrm{F}}\left(\phi(\mathbf{x},t),c(\mathbf{x},t)\right) = \frac{\chi\left(\phi(\mathbf{x},t),c(\mathbf{x},t)\right)}{f\left(\phi(\mathbf{x},t)\right)}$$

The friction coeffiecient is given as

$$f\left(\phi(\mathbf{x},t)\right) = 6\pi\eta_{\mathrm{w}} r_{\mathrm{eq}} + V_{\mathrm{p}} k_0 \tau^2 a_{\mathrm{p}}^2 \eta_{\mathrm{w}} \frac{\phi(\mathbf{x},t)}{\left(1-\phi(\mathbf{x},t)\right)^2}$$

where r_{eq} for coin-like particles can be written as

$$r_{\mathrm{eq}} = \frac{\dfrac{\delta_p}{2}\sqrt{\dfrac{4S_{\mathrm{p}}}{\pi\delta_{\mathrm{p}}^2}-1}}{\tan^{-1}\left(\sqrt{\dfrac{4S_{\mathrm{p}}}{\pi\delta_{\mathrm{p}}^2}-1}\right)}$$

The χ function can be written as

$$\chi(\mathbf{x},t) = \chi\left(\phi(\mathbf{x},t),c(\mathbf{x},t)\right) = k_{\mathrm{B}}T + (h(\mathbf{x},t)+\delta_{\mathrm{p}})^2\left(\frac{\partial F_{\mathrm{A}}}{\partial h} - \frac{\partial F_{\mathrm{R}}}{\partial h}\right)$$

where h is the separation between the flat particles

$$h(\mathbf{x},t)=h(\phi(\mathbf{x},t))=\frac{\phi_{\max}\delta_{\mathrm{p}}}{\phi(\mathbf{x},t)}-\delta_{\mathrm{p}}=\left(\frac{\phi_{\max}}{\phi(\mathbf{x},t)}-1\right)\delta_{\mathrm{p}}$$

F_A represents the van der Waals attractive and F_R the electrical repulsive forces:

$$F_{\mathrm{A}}(\mathbf{x},t)=F_{\mathrm{A}}(\phi(\mathbf{x},t))=\frac{A_{\mathrm{H}}S_{\mathrm{p}}}{6\pi}\left(\frac{1}{h(\mathbf{x},t)^3}-\frac{2}{(h(\mathbf{x},t)+\delta_{\mathrm{p}})^3}+\frac{1}{(h(\mathbf{x},t)+2\delta_{\mathrm{p}})^3}\right)$$

and

$$\frac{\partial F_{\mathrm{A}}(\phi(\mathbf{x},t))}{\partial h}=-\frac{A_{\mathrm{H}}S_{\mathrm{p}}}{2\pi}\left[\frac{1}{h(\mathbf{x},t)^4}-\frac{2}{(h(\mathbf{x},t)+\delta_{\mathrm{p}})^4}+\frac{1}{(h(\mathbf{x},t)+2\delta_{\mathrm{p}})^4}\right]$$

The electric double layer force term is given by

$$F_{\mathrm{R}}(\mathbf{x},t)=F_{\mathrm{R}}(\phi(\mathbf{x},t),c(\mathbf{x},t))=2c(\mathbf{x},t)RTS_{\mathrm{p}}(\cosh y^{\mathrm{m}}(\mathbf{x},t)-1)$$

which derivative respect to h is

$$\frac{\partial F_{\mathrm{R}}(\mathbf{x},t)}{\partial h}=\frac{\partial F_{\mathrm{R}}(\phi(\mathbf{x},t),c(\mathbf{x},t))}{\partial h}=-4\kappa c(\mathbf{x},t)RTS_{\mathrm{p}}\tanh y^{\mathrm{m}}(\mathbf{x},t)$$
$$\times\left[\cosh y_{\infty}^{\mathrm{m}}(\mathbf{x},t)\sinh\left(\frac{y_{\infty}^{\mathrm{m}}(\mathbf{x},t)}{2}\right)+\frac{1}{\kappa(\mathbf{x},t)h(\mathbf{x},t)}\sinh y_{\infty}^{\mathrm{h}}(\mathbf{x},t)+\frac{2}{(\kappa(\mathbf{x},t)h(\mathbf{x},t))^2}\sinh\left(\frac{y_{\infty}^{\mathrm{h}}(\mathbf{x},t)}{2}\right)\right]$$

where

$$y^{\mathrm{m}}(\mathbf{x},t)=\sinh^{-1}\left[2\sinh y_{\infty}^{\mathrm{m}}(\mathbf{x},t)+\frac{4}{\kappa(\mathbf{x},t)h(\mathbf{x},t)}\sinh\left(\frac{y_{\infty}^{\mathrm{h}}(\mathbf{x},t)}{2}\right)\right]$$

$$y_{\infty}^{\mathrm{m}}(\mathbf{x},t)=4\tanh^{-1}\left[\tanh\left(\frac{y_{\infty}^{0}(\mathbf{x},t)}{4}\right)\exp\left(-\kappa(\mathbf{x},t)h(\mathbf{x},t)/2\right)\right]$$

$$y_{\infty}^{\mathrm{h}}(\mathbf{x},t)=4\tanh^{-1}\left[\tanh\left(\frac{y_{\infty}^{0}(\mathbf{x},t)}{4}\right)\exp\left(-\kappa(\mathbf{x},t)h(\mathbf{x},t)\right)\right]$$

The surface potential of an isolated plate is given by

$$y_{\infty}^{0}(\mathbf{x},t)=y_{\infty}^{0}(c(\mathbf{x},t))=2\sinh^{-1}\left(\frac{zF\sigma^{0}}{2\varepsilon_0\varepsilon_{\mathrm{r}}\kappa(\mathbf{x},t)RT}\right)$$

where κ is the reciprocal Debye length

$$\kappa(\mathbf{x},t)=\kappa(c(\mathbf{x},t))=\sqrt{\frac{2c(\mathbf{x},t)F^2}{\varepsilon_0\varepsilon_r RT}}$$

The transmissivity of a fracture is

$$T(\mathbf{x},t)=T(\phi(\mathbf{x},t),c(\mathbf{x},t))=T_w\frac{\eta_w}{\eta(\mathbf{x},t)}$$

and Darcy's law is written as

$$S\frac{\partial p(\mathbf{x},t)}{\partial t}=\nabla\cdot\left[T(\phi(\mathbf{x},t),c(\mathbf{x},t))\nabla p(\mathbf{x},t)\right]$$

and Darcy velocity is

$$\mathbf{u}(\mathbf{x},t)=-T(\phi(\mathbf{x},t),c(\mathbf{x},t))\nabla p(\mathbf{x},t)$$

η is the viscosity of the fluid, which depends on ϕ and c

$$\eta(\phi,c)=\eta_w\left[1+1.022\phi_{\mathrm{cov}}(\phi,c)+1.358\phi_{\mathrm{cov}}^3(\phi,c)\right]$$

Where ϕ_{cov} is a co-volume fraction

$$\phi_{\mathrm{cov}}(\mathbf{x},t)=\phi_{\mathrm{cov}}(\phi(\mathbf{x},t),c(\mathbf{x},t))=\frac{2}{3}\frac{\left(D_p+\frac{2m}{\kappa(\mathbf{x},t)}\right)^3}{D_p^2\delta_p}\phi$$

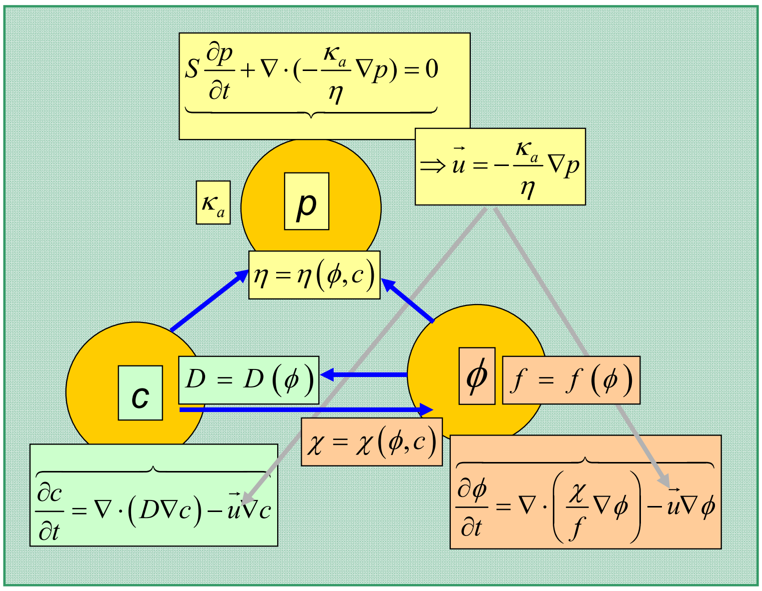

Figure A1. *Mutual couplings of model variables.*

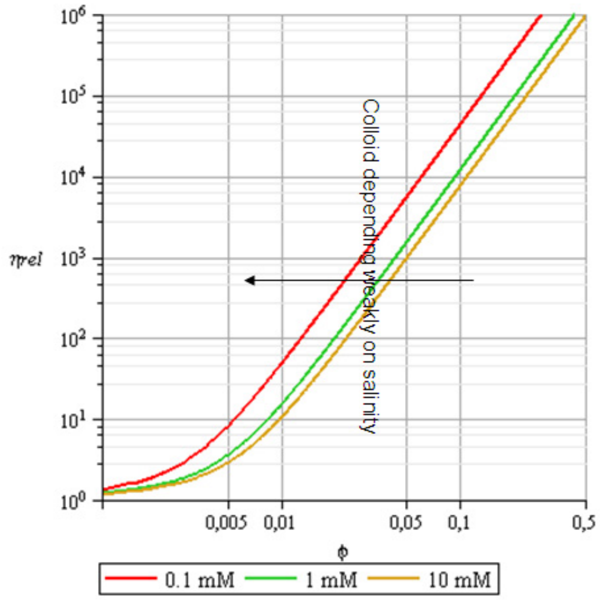

Figure A2. *Relative viscosity as a function of bentonite volume fraction at three different ionic strengths.*

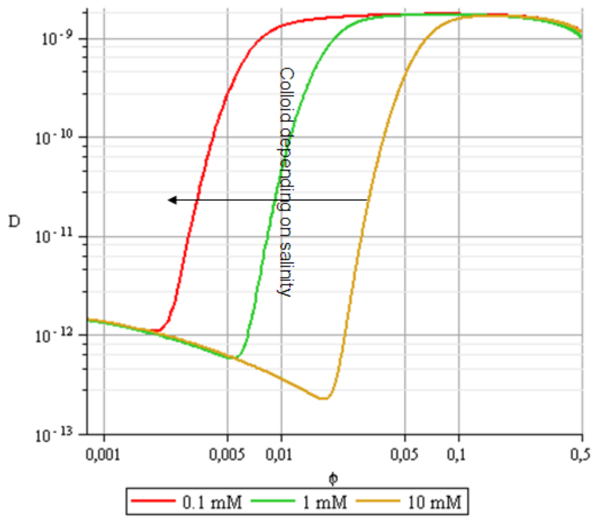

Figure A3. *Diffusivity D_F (y-axis, m^2/s) as a function of volume fraction at three different ionic strengths (log-log scaling). Note how the diffusivity decreases as the bentonite changes to colloidal form (at the same time also concentration or volume fraction is low).*

Table A1. *Nomenclature, and parameter values, if fixed.*

Notation	Property	value and/or unit
k_B	Boltzmann's constant	$1.380 \cdot 10^{-23}$ J/K
S	Capacity factor for groundwater flow	1
D_0	Diffusion coefficient of ions in free water.	$2 \cdot 10^{-9}$ m^2/s
r_{eq}	Equivalent radius of non-spherical particles	m
F	Faraday's constant	96 485 C/mol
m	Fitting parameter in co-volume fraction	1
δ	Fracture aperture	1 mm (typically)
R	Gas constant	8.314 J/(K mol)
A_H	Hamaker constant	$2.5 k_B T$
$k_0 \tau^2$	Kozenys' constant	5, 13[(1]
ϕ_{max}	Maximum volume fraction of smectite	1
c	Na-concentration - variable	mol/m^3 or mM
c_0	Na-concentration in groundwater	0.1 mM
C_0	Na-concentration in porewater	10 mM
ε_0	permittivity of vacuum	$8.854 \cdot 10^{-12}$ F/m
ε_r	Relative permittivity of water	78.54
D_p	Smectite particle diameter	200 nm
δ_p	Smectite particle thickness	$1 \cdot 10^{9}$ m
ρ_S	Specific density of smectite	2 750 kg/m^3
ρ_w	Specific density of water	1 000 kg/m^3
a_p	Specific surface area per unit volume of particles	m^2/m^3
S_p	Surface area of smectite particle	1
σ^0	Surface charge of particles	-0.131 C/m^2
T	Temperature	298.15 K
T_w	Transmissivity of water conducting fracture	m^2/s
z	Valence of counterion	1
η_w	Viscosity of water	$1.002 \cdot 10^{-3}$ Ns/m^2
ϕ	Volume fraction of smectite - variable	1
V_P	Volume of the smectite particles	m^3
p	Water pressure in the fracture - variable	Pa

Appendix B: The equations in BESW_S model of VTT

As mentioned in Section 2.1 the original equation of Neretnieks et al. (2009) model are quite difficult to implement, as they include several nested function calls and that it is an open question which dependencies are causing the observed numerical problems.

In order to enhance numerical computation in COMSOL Multiphysics, we have simplified some functional dependencies. All simplifications are based on relatively simple analytical relations, for which first order partial derivatives are also available.

The needed processes and their related parameters are shown in Table B1. Note that while volume fraction affects all three transport parameters and concentration two, the pressure has no effect via transport parameters.

Table B1. *The processes, variables and transport parameters applied in BESW-model. The units, mutual dependencies and variable names applied in COMSOL are also shown.*

Process	Name	Unit	Transport parameter	Name	Unit	Dep. on *c*	Dep. on ϕ	Dep. on *p*
Diffusion of sodium, concentration	*c*	mol/m^3	Diffusion coefficient	*D*	m^2/s	no	yes	no
Transport smectite, volume fraction	ϕ	-	Diffusion coefficient	D_F	m^2/s	yes	yes	no
Darcy flow, pressure	*p*	Pa	Viscosity	η_{rel}	1	yes	yes	no

For relative viscosity Neretnieks et al. (2010) apply formula

$$\eta_{\text{rel}} = \frac{\eta}{\eta_w} = 1 + a_1\phi_{\text{cov}} + a_3\phi_{\text{cov}}^3$$

$$a_1 = 1.022$$

$$a_1 = 1.358$$

Where ϕ_{cov} is a co-volume fraction

$$\phi_{\text{cov}} = \frac{2}{3}\frac{\left(D_{\text{p}} + 2m\kappa^{-1}\right)^3}{D_{\text{p}}^2\delta_{\text{p}}}\phi$$

and, therefore relative viscosity fully out written

$$\eta_{\text{rel}} = 1 + a_1\frac{2}{3D_{\text{p}}^2\delta_{\text{p}}}\left(D_{\text{p}} + \frac{1}{F}\sqrt{\frac{2\varepsilon\varepsilon_0 RT}{c}}\right)^3\phi + a_3\left(\frac{2}{3D_{\text{p}}^2\delta_{\text{p}}}\right)^3\left(D_{\text{p}} + \frac{1}{F}\sqrt{\frac{2\varepsilon\varepsilon_0 RT}{c}}\right)^9\phi^3$$

In a more suitable formulation for COMSOL or any numerical calculations, the equation may be written as

$$\eta_{\text{rel}} = 1 + k_5 \left(1 + \sqrt{\frac{k_7}{c}}\right)^3 \phi + k_6 \left(1 + \sqrt{\frac{k_7}{c}}\right)^9 \phi^3 = 1 + k_5\, \beta(c)^3 \phi + k_6\, \beta(c)^9 \phi^3$$

where

$$\beta(c) = 1 + \sqrt{\frac{k_7}{c}}$$

$$k_5 = a_1 \frac{2D_{\text{p}}}{3\delta_{\text{p}}}$$

$$k_6 = a_3 \left(\frac{2D_{\text{p}}}{3\delta_{\text{p}}}\right)^3$$

$$k_7 = \frac{2\varepsilon\varepsilon_0 RT}{D_{\text{p}}^2 F^2}$$

Values for parameters in most applied case (particle diameter 250 nm and thickness 1 nm)

$$\delta_{\text{p}} = 10^{-9}\,\text{m}$$

$$D_{\text{p}} = 250 \times 10^{-9}\,\text{m}$$

$$k_5 = 170.33$$

$$k_6 = 6.287 \times 10^6$$

$$k_7 = 5.922 \times 10^{-3}$$

The model equations given for smectite diffusion by Moreno et al. (2010) are quite complex set of composite functions. Therefore, we tried to fit something not so complicated especially to diffusion function, which is behaves quite non-linearly as function of salinity (ionic strength) and volume fraction of smectite.

Our conceptual thinking is sketched in Figure B1, where the diffusivity is shown as a function of ϕ at four salinity levels. There is some high diffusivity value D_{F}^{h} which is reached by all salinity values when ϕ is high enough (> 0.1). At low ϕ values the behaviour is more complicated due to the minimum value of diffusivity at salinity dependent ϕ values. It is though logical and even physically reasonable to consider two distinct diffusivity functions: one for colloidal diffusion ($D_{\text{F}}^{\text{c}}(c)$) and one for gel like smectite. Therefore, we try to find function α for following fit of smectite diffusivity.

$$D_{\text{F}}(\phi, c) = D_{\text{F}}^{\text{l}} \cdot \left(\frac{D_{\text{F}}^{\text{h}}}{D_{\text{F}}^{\text{l}}}\right)^{\alpha(\phi, \phi_{\text{t}}(c))} + D_{\text{F}}^{\text{c}}(c)$$

We have chosen for function α (see parameter values in Table B2)

$$\alpha(\phi,c)=\frac{1}{1+\left(\dfrac{\ln\phi}{\ln A+b\ln c}\right)^{n}}$$

Full diffusivity function looks like this fully out-written

$$D_{\mathrm{F}}(\phi,c)=D_{\mathrm{F}}^{\mathrm{l}}\cdot\left(\frac{D_{\mathrm{F}}^{\mathrm{h}}}{D_{\mathrm{F}}^{\mathrm{l}}}\right)^{\left(1+\left(\frac{\ln\phi}{\ln\left(Ac^{b}\right)}\right)^{n}\right)^{-1}}+D_{\mathrm{F}}^{\mathrm{c}}=D_{\mathrm{F}}^{\mathrm{l}}\cdot\left(\frac{D_{\mathrm{F}}^{\mathrm{h}}}{D_{\mathrm{F}}^{\mathrm{l}}}\right)^{\left(1+\left(\frac{\ln\phi}{\ln A+b\ln c}\right)^{n}\right)^{-1}}+D_{\mathrm{F}}^{\mathrm{c}}$$

or by α function

$$D_{\mathrm{F}}(\phi,c)=D_{\mathrm{F}}^{\mathrm{l}}\cdot\left(\frac{D_{\mathrm{F}}^{\mathrm{h}}}{D_{\mathrm{F}}^{\mathrm{l}}}\right)^{\alpha(\phi,c)}+D_{\mathrm{F}}^{\mathrm{c}}=D_{\mathrm{F}}^{\mathrm{l}}\cdot\left(\frac{D_{\mathrm{F}}^{\mathrm{h}}}{D_{\mathrm{F}}^{\mathrm{l}}}\right)^{\alpha(\phi,c)}+D_{\mathrm{F}}^{\mathrm{c}}$$

Table B2. *Parameters*

Parameter	Value	Unit
n	16	-
A	0.009± 3.90E-005	-
b	0.492± 0.0020	-
$D_{\mathrm{F}}^{\mathrm{h}}$	1.6e-9	m^2/s
$D_{\mathrm{F}}^{\mathrm{l}}$	1e-13	m^2/s
$D_{\mathrm{F}}^{\mathrm{c}}$	1.9e-12	m^2/s

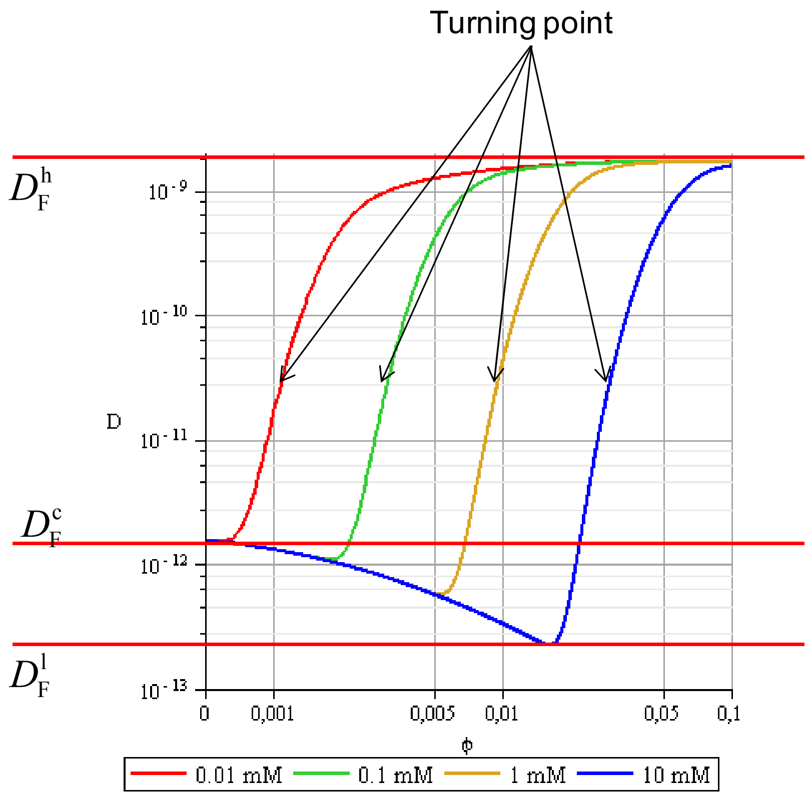

Figure B1. *Diffusivity of smectite as a function of volume fraction of smectite (phi) and salinity (ionic strength). At the four ionic strengths shown, the diffusivity curve has a distinct turning point, before which diffusivity is low and which it high. The location of turning points depends on salinity.*

Appendix C: Model implementations

In order to make the model hierarchy clearer, we have produced Figure C1.

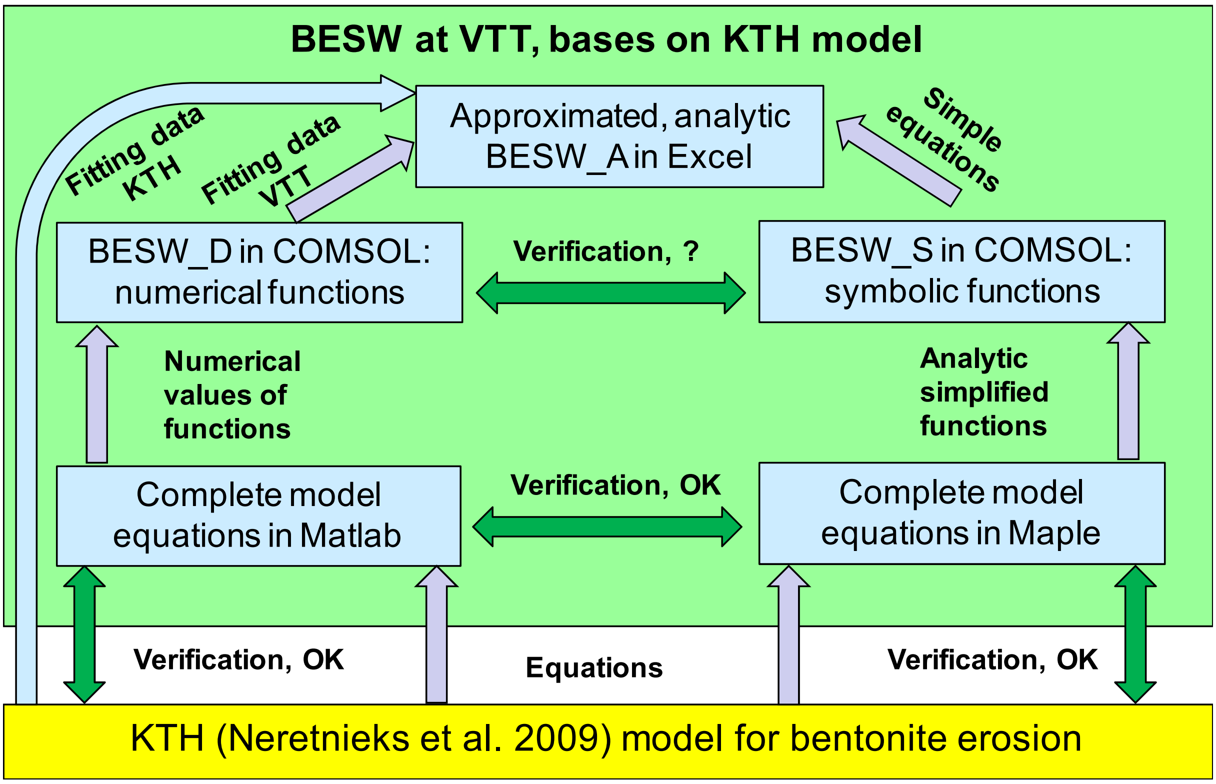

Figure C1. *Coupling between original Neretnieks' model and VTT's different implementations. Note, that BESW_A model applied in this work is fitted to original KTH data.*